Bioorganic & Medicinal Chemistry Letters 22 (2012) 5326–5329

Contents lists available at SciVerse ScienceDirect

Bioorganic & Medicinal Chemistry Letters

journal homepage: www.elsevier.com/locate/bmcl

Pyrimidinopyrimidine inhibitors of ketohexokinase: Exploring the ring C2 group that interacts with Asp-27B in the ligand binding pocket

Bruce E. Maryanoff *,†, John C. O'Neill, David F. McComsey, Stephen C. Yabut, Diane K. Luci, Alan C. Gibbs, Margery A. Connelly *

Janssen Pharmaceutical Companies of Johnson & Johnson, Welsh & McKean Roads, Spring House, PA 19477-0776, United States

ARTICLE INFO

Article history:
Received 13 March 2012
Revised 1 June 2012
Accepted 4 June 2012
Available online 17 June 2012

Keywords:
Kinase
Diabetes
Obesity
Fructose metabolism

ABSTRACT

Inhibitors of ketohexokinase (KHK) have potential for the treatment of diabetes and obesity. We have continued studies on a pyrimidinopyrimidine series of potent KHK inhibitors by exploring the 2-position substituent (R^3) that interacts with Asp-27B in the ATP-binding region of KHK (viz. **1**, **2**; Table 1). We found that increased spacing between the terminal ammonium group and the heterocyclic scaffold (viz. **16**–**20**), such that interaction with Asp-27B is not possible, still results in potent KHK inhibition (IC_{50} = 15–50 nM). We propose a new interaction with Asp-194, which serves to expand the pyrimidinopyrimidine pharmacophore.

Elevated fructose ingestion promotes various metabolic disturbances in animal models, including weight gain, hyperlipidemia, hypertension, and insulin resistance.[1–5] Furthermore, the long-term consumption of fructose in overweight humans increases energy intake, body weight, fat mass, blood pressure, and plasma triglycerides.[6,7] This situation exacerbates, and contributes to the onset of, non-insulin-dependent (type 2) diabetes mellitus (NIDDM), which is characterized by hyperglycemia and insulin resistance. Indeed, a marked correlation exists between the prevalence of NIDDM and increased energy intake from highly refined sugars.[8]

The enzyme ketohexokinase (KHK; EC 2.7.1.3), also known as fructokinase, rapidly metabolizes fructose within the liver.[9] KHK catalyzes the phosphorylation of fructose on position C1 by transferring a phosphate group from adenosine 5′-triphosphate (ATP) to yield fructose-1-phosphate (F1P), which enters normal metabolic pathways.[10–12] Unfortunately, fructose metabolism lacks robust control mechanisms, unlike the tight regulation of glucose pathways.[13] Given that KHK has a high K_M value, is not inhibited by product (F1P), and is not regulated allosterically, high concentrations of fructose can readily provide the components of triglycerides.[14] Support for KHK as a therapeutic target emanates from human genetic mutations that cause essential fructosuria.[15] In this benign condition, individuals have inactive isoforms of hepatic KHK, such that ingestion of fructose, sucrose, or sorbitol imparts elevated blood fructose levels and increased urinary excretion of fructose. Consequently, the targeting of fructose metabolism by inhibition of KHK could offer a novel approach to treat NIDDM and obesity amidst modern diets due to reduced body weight, free fatty acids, and triglycerides, without a mechanism-based safety issue.

We recently reported a series of pyrimidinopyrimidine derivatives that provide potent, selective inhibitors of human hepatic KHK (KHK-C isoform).[16] For example, **1** exhibited a KHK IC_{50} value of 12 nM and showed good cellular KHK inhibition (IC_{50} <500 nM). An X-ray cocrystal structure of **1**·KHK, a functional pseudo-homodimer (*a* and *b* subunits) with each subunit occupied by the ligand, revealed important interactions within the enzyme's ATP-binding pocket, one of which involved the side chain of Asp-27B (Fig. 1).[16] Because this ionic interaction seems particularly important for anchoring the ligand and achieving high affinity, we have explored it more thoroughly, as depicted by the red atoms in structure **2**. The results of this investigation are reported herein.

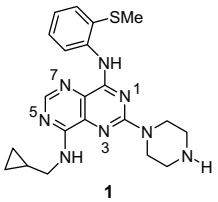

1

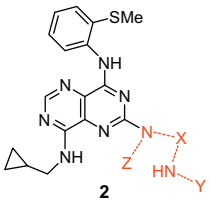

2

* Corresponding authors. Tel.: +1 267 980 3512 (B.E.M.); tel.: +1 215 628 5202 (M.A.C.).

E-mail addresses: bmaryano@scripps.edu (B.E. Maryanoff), mconnell@its.jnj.com (M.A. Connelly).

† Present addresses: Department of Chemistry, The Scripps Research Institute, 10550 North Torrey Pines Road, La Jolla, CA 92037, USA. Pennsylvania Drug Discovery Institute, 3805 Old Easton Road, Doylestown, PA 18902, USA.

0960-894X/$ - see front matter © 2012 Elsevier Ltd. All rights reserved.
http://dx.doi.org/10.1016/j.bmcl.2012.06.008

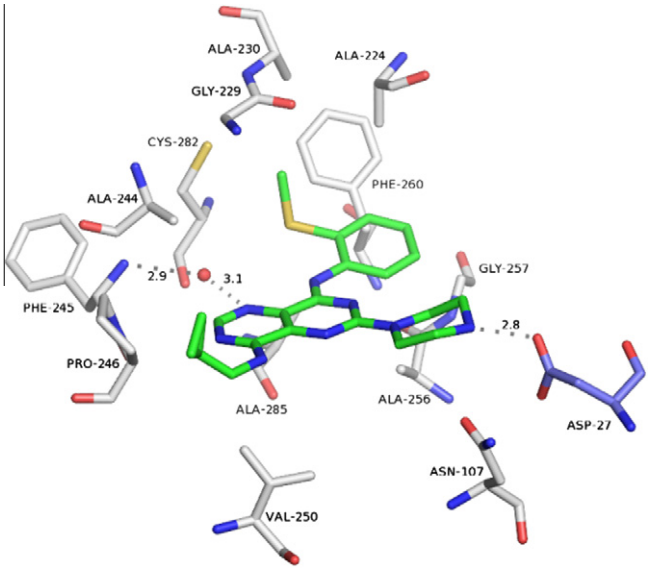

Figure 1. Crystal structure of the **1**·KHK complex. View of **1** (C, green; N, blue; S, yellow) and neighboring KHK residues in subunit *a* (C, white; N, blue; O, red; S, yellow) with Asp-27 in subunit *b* ('Asp-27B') (C, light blue; N, blue; O, red). The red sphere represents a conserved water molecule. The H-bond between the piperazine nitrogen and Asp-27B Oδ is 2.8 Å (PDB accession number: 3Q92).

The 2-(methylthio)phenylamino group was found to be optimal at position 8 (viz. **1**) and cyclopropylmethylamino was among the best groups at position 4.[15] Since the Asp-27B residue of KHK is located in the vicinity of the polar channel through which the triphosphate moiety of ATP passes, we supposed that additional, useful interactions could be obtained by modifying the substituent at position 2 (R^3), especially by extension into the 'triphosphate channel' (Fig. 2). As reported earlier,[15] the piperazino group can be successfully replaced by 3-aminopiperidino, 4-(aminomethyl)piperidino, 3-(aminomethyl)piperidino, 3-(aminomethyl)azetidino, and 2,6-diazaspiro[3.3]hept-2-yl [3,3′-spiro(bis-azetidin)-1-yl; **3**] groups, maintaining good potency (IC_{50} = 8–30 nM); thus, the spacing between the Asp-27B interactive nitrogen and the heterocyclic scaffold is not narrowly defined. However, the acyclic R^3 group $MeNHCH_2CH_2(Me)N$- was not as effective, with an IC_{50} of 130 nM. An ammonium group bearing more than one proton, that is NH_2^+ or NH_3^+, appeared to be optimal for interaction with Asp-27B. For example, the N-methylpiperazino analogue of **1** was 10-fold less potent than **1** (IC_{50} = 110 nM).

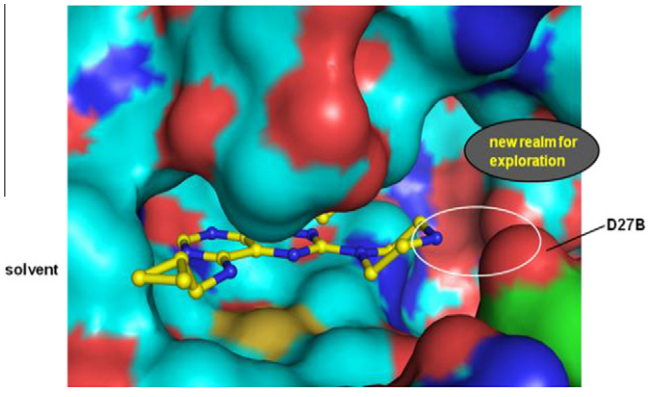

Figure 2. Crystal structure of the **1**·KHK complex (mainly subunit *a*) depicting the D27B interaction (open ellipse) and the potentially useful channel domain (filled ellipse). Color code: C, light blue; N, blue; O, red; S, yellow; C in subunit *b*, green.

Table 1
Structures and KHK inhibition results for analogues of **1** with variation of so-called R^3

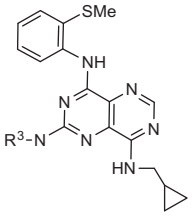

Compd[a]	N-R^3 [b]	IC_{50}[c] (nM)
1	Piperazino	12
3	2,6-Diazaspiro[3.3]hept-2-yl	8.0
4	3-Me-piperazino	70
5	(*R*)-2-Me-piperazino	58
6	*cis*-2,6-diMe-piperazin-4-yl	110
7	3,3-di-Me-piperazino	40
8	(piperidin-4-yl)CH_2NMe–	66
9	(*R,R*)-*cis*-H8-6*H*-Pyrrolo[3,4-*b*]pyridin-6-yl	440
10	(*S,S*)-*cis*-H8-6*H*-Pyrrolo[3,4-*b*]pyridin-6-yl	300
11	(*S,S*)-2,5-Diazabicyclo[2.2.1]hept-2-yl	4600
12	(3-Amino-8-aza-bicyclo[3.2.1]octan)-8-yl	800
13	2,3,4,5-Tetrahydro-1*H*-1,4-benzodiazepin-4-yl	6000
14	3,3′-Spiro(bis-pyrrolidin)-1-yl	43
15	2,6-Diazaspiro[3.4]octan-6-yl	2.0
16	4,4′-Spiro(bis-piperidin)-1-yl	15
17	4-(Piperidin-4-yl)piperazino	48
18	4-(Piperazin-1-yl)piperidino	28
19	4-(Piperidin-4-yl)piperidino	50
20	4-(4-Me-piperazin-1-yl)piperidino	30

[a] New compounds were purified by HPLC and characterized by ESI-MS and ^1H NMR.
[b] The term 'R^3' relates to the substituent on position 2 (i.e., C2) of the pyrimidinopyrimidine scaffold, as used in Ref. 6.
[c] Inhibition of recombinant human hepatic KHK in terms of IC_{50} values.

Further exploration of this portion of the ligand was carried out with compounds **4**–**19** (Table 1; Chart 1). The compounds of interest were synthesized by using key starting material **21**,[16] as exemplified for production of **14** (Scheme 1), and assayed for inhibition of human hepatic KHK (KHK-C) according to the method described earlier.[16]

Analogues **4**–**7** were meant to test the effect of C-methylation of the piperazine ring, the distal nitrogen of which binds to Asp-27B. A single methyl group adjacent to the interacting piperazine nitrogen resulted in a sixfold loss of potency (cf. **4** and **1**) and a single, remote methyl group resulted in fivefold loss in potency (cf. **5** and **1**). Two methyl groups adjacent to the interacting piperazine nitrogen, on opposite sides, resulted in a ninefold loss of potency (cf. **6** and **1**) and *gem*-dimethyl groups resulted in just a threefold loss of potency (cf. **7** and **1**). These data indicate that moderate steric hindrance in this part of the ligand is not a major impediment to effective KHK binding. However, bicyclic piperazine **11** led to a nearly 400-fold loss in potency (cf. **11** and **1**) and bulky bicyclic amine **12** was much less potent (cf. **12** and **1**). A fused phenyl ring that decreased the basicity of the interactive nitrogen was very disruptive (cf. **13** and **1**).

As noted above, additional spacing between the Asp-27B interactive nitrogen and the pyrimidinopyrimidine scaffold, such as with 4-(aminomethyl)piperidine (KHK IC_{50} = 10 nM), still afforded potent KHK inhibition. Reversal of the connectivity, as in **8**, was also reasonably well tolerated (IC_{50} = 66 nM). However, conformational constraint, as with **9** and **10**, resulted in a 30-fold reduction in potency. Because the use of a spirocyclic piperazine-mimetic, as in **3**, provided very potent KHK inhibition (IC_{50} = 8 nM), we explored this approach further with compounds **14**–**16**, which gave good KHK inhibition. Indeed, compound **15**, with an IC_{50} value of 2 nM, has the distinction of being the most potent substance yet

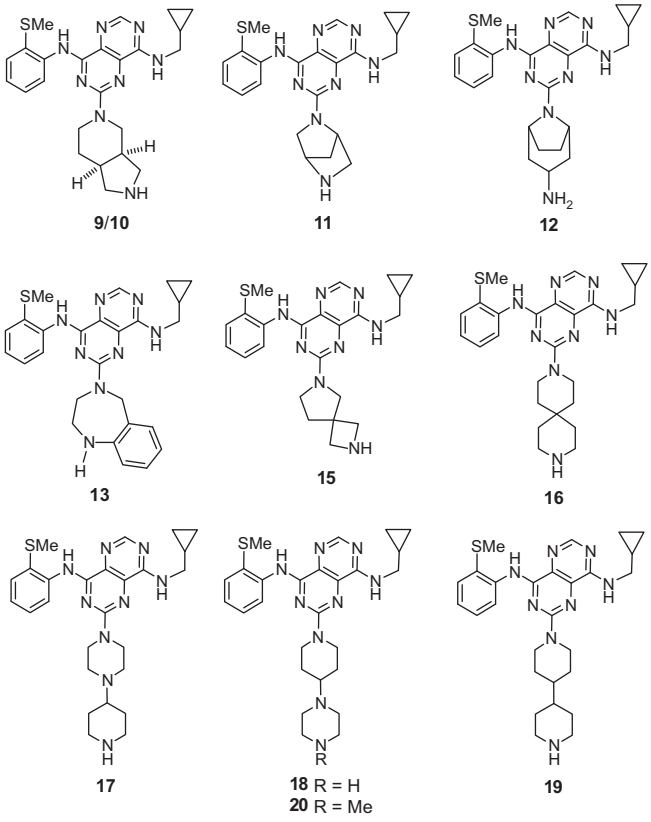

Chart 1.

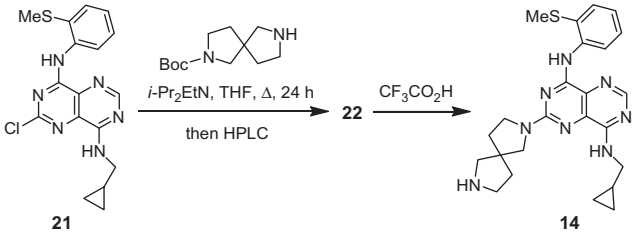

Scheme 1.

reported for inhibition of KHK (fourfold better than **3**).[16–18] The high potency for **16** (IC_{50} = 15 nM) was surprising, since the interactive nitrogen atom is now positioned well beyond the region of the active site that is dominated by Asp-27B. Additional studies with **17**–**19** confirmed this point, with IC_{50} values ranging from 30 to 50 nM. Moreover, methylation of the terminal nitrogen of **18** did not cause a significant loss in potency (viz. **20**), which differs from the above-mentioned 10-fold loss for N-methylation of **1**. These results suggest that a different KHK carboxylate residue may be involved.

We sought to explain the observations with **16**–**20** by obtaining a ligand-KHK cocrystal structure. However, we were unable to grow suitable crystals with **16**, **17**, or **18**, perhaps due to conformational changes in the protein sufficient to alter the original crystallization mode. Therefore, we resorted to a computational docking study with **18** in the closed subunit (*a*) of KHK to acquire some understanding (Fig. 3).[17,19] Ligand **18** is oriented in the active site of KHK is the usual manner,[16] except that the terminal ammonium group of the now-extended R^3 group (i.e., the piperazine nitrogen) is not in the vicinity of Asp-27B to interact with its carboxylate side chain. By contrast, that ammonium group of **18** is poised to interact

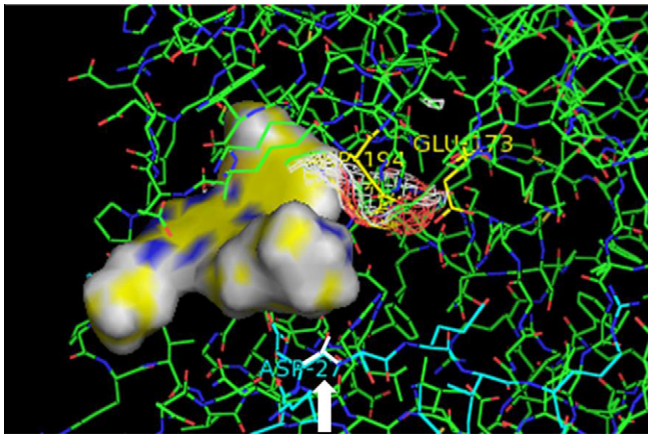

Figure 3. Computer docking model of **18** (mostly grayish white and yellow Connolly surface; N, blue) complexed with KHK (mainly subunit *a*; stick model: C, green; N, blue; O, red; C in subunit *b*, light blue) depicting the Asp-194 interaction (yellow side chain; red, hashed Connolly surface). Acid residues Asp-27B (white side chain with white arrow below it) and Glu-173 (yellow side chain), which are out of reach of the piperazine NH_2^+ group, are also labeled.

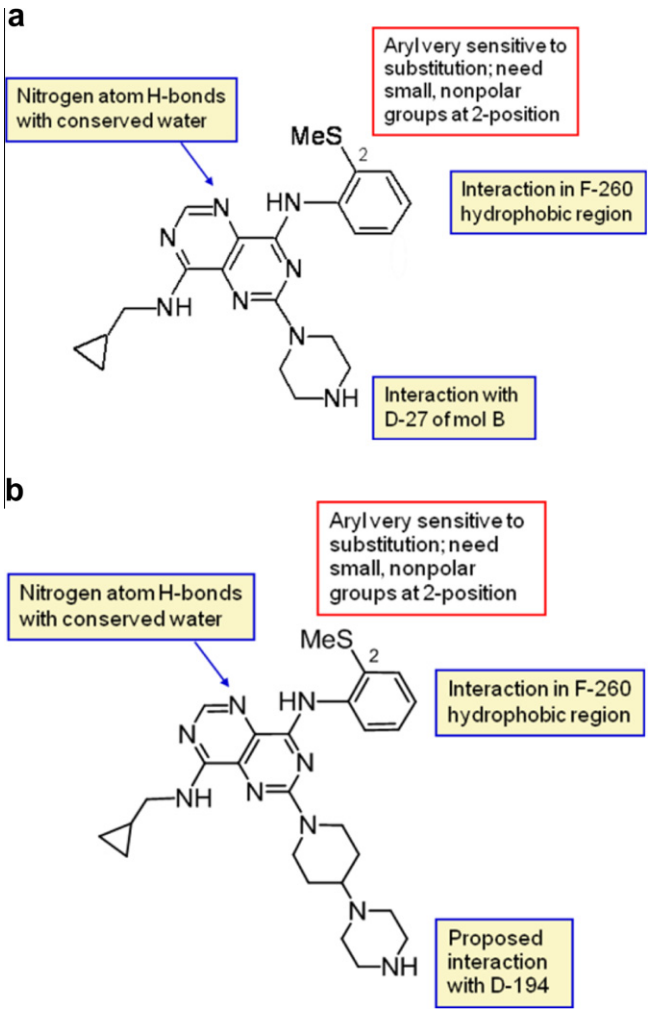

Figure 4. Schematic diagrams showing the key pharmacophore requirements for (**a**) **1** and (**b**) **18**.

with the carboxylate side chain of Asp-194 within the triphosphate channel. The carboxylate side chain of Glu-173, another potential site for interaction, is too remote to be accessed. If the modeling

picture proposed for **18** is valid, then compounds **16**, **17**, **19**, and **20** would presumably adopt this new interaction mode, as well.

An alternative explanation for the high potency of **16**–**20** could derive from considering binding of the ligand in the active site of KHK subunit *b*, which has a very 'open' conformation.[16] However, an inspection of this active-site cavity did not reveal an obvious acid residue at a favorable location for enhancing ligand affinity.

Given the excellent KHK inhibition for **15**, it was studied in a HepG2 cellular assay that measures the level of fructose-1-phosphate in cell lysates by using LC–MS for quantification.[16] Compound **15** exhibited potent cellular KHK inhibition, with an IC_{50} value of 150 nM.

Compound **17** was examined in a diverse panel of 31 human protein kinases, representing the different families, for off-target kinase inhibition at a concentration of 10 μM (Invitrogen; with 100 μM ATP).[20] None of the 31 kinases was inhibited >50% at this high concentration of **17**. CAMK2A was inhibited by 41% at 10 μM, but the rest were inhibited <15% (IC_{50} <<10 μM for 30 kinases). Compound **3** did not inhibit any of these kinases by more than 25% at 10 μM.

Our original study on pyrimidinopyrimidines[16] was the first published report of potent KHK inhibitors (IC_{50} <100 nM). The pharmacophore was established by X-ray data, such as for **1**·KHK: in the *a* subunit of KHK, the ring nitrogen N3 of the pyrimidinopyrimidine was hydrogen bonded to the conserved water molecule, the 2-(methylthio)phenyl group occupied a hydrophobic region largely defined by Phe-260, and the piperazine NH_2^+ (of R^3) interacted with the carboxylate side chain of Asp-27B (Fig. 4a). Our present study suggests an expansion of the pharmacophore for potent KHK inhibition, wherein the terminal ammonium group of **16**–**20** now extends beyond the reach of Asp-27B to interact with Asp-194, as represented in Figure 4b. Thus, it would appear that the R^3 substituent can be substantially augmented, as in **16**–**20**, while retaining a high level of KHK affinity. Other KHK inhibitor ligands, identified through fragment-based methods, further illustrate the possible modes of interaction within the ATP-binding pocket of KHK based on different chemotypes.[17,18]

In summary, we have studied the pyrimidinopyrimidine series of KHK inhibitors further by exploring the substituent at ring position 2 (referred to as R^3) that interacts with Asp-27B in the ligand binding pocket. We found that the R^3 group can be substantially enlarged while retaining potent KHK inhibition, as with analogues **16**–**20**. Given the extended spacing of the terminal ammonium group away from the pyrimidinopyrimidine scaffold, interaction with Asp-27B is not possible; however, a new, putative interaction with Asp-194 is introduced. This finding not only further defines the pyrimidinopyrimidine pharmacophore for obtaining potent KHK inhibition, but also suggests a potential interaction site for other KHK inhibitor chemotypes.

Acknowledgments

We thank Dr. Marta Abad for helpful discussions; Dr. John Masucci and William Jones for LC–MS analysis.

References and notes

1. Kasim-Karakas, S. E.; Vriend, H.; Almario, R.; Chow, L. C.; Goodman, M. N. *J. Lab. Clin. Med.* **1996**, *128*, 208.
2. Hwang, I. S.; Ho, H.; Hoffman, B. B.; Reaven, G. M. *Hypertension* **1987**, *10*, 512.
3. Reiser, S.; Hallfrisch, J. *J. Nutr.* **1977**, *107*, 147.
4. Zavaroni, I.; Sander, S.; Scott, S.; Reaven, G. M. *Metabolism* **1980**, *29*, 970.
5. Martinez, F. J.; Rizza, R. A.; Romero, J. C. *Hypertension* **1994**, *23*, 456.
6. Raben, A.; Vasilaras, T. H.; Moller, A. C.; Astrup, A. *Am. J. Clin. Nutr.* **2002**, *76*, 721.
7. Teff, K. L.; Elliott, S. S.; Tschop, M.; Kieffer, T. J.; Rader, D.; Heiman, M.; Townsens, R. R.; Keim, N. L.; D'Alessio,; Havel, P. J. *J. Clin. Endocrinol. Metab.* **2004**, *89*, 2963.
8. Gross, L. S.; Li, L.; Ford, E. S.; Liu, S. *Am. J. Clin. Nutr.* **2004**, *79*, 774.
9. Basciano, H.; Federico, L.; Adeli, K. *Nutr. Metab.* **2005**, *2*, 5. http://dx.doi.org/10.1186/1743-7075-2-5.
10. Raushel, F. M.; Cleland, W. W. *Biochemistry* **1977**, *16*, 2169.
11. Raushel, F. M.; Cleland, W. W. *Biochemistry* **1977**, *16*, 2176.
12. Raushel, F. M.; Cleland, W. W. *J. Biol. Chem.* **1973**, *248*, 8174.
13. Mayes, P. A. *Am. J. Clin. Nutr.* **1993**, *58*, 754S.
14. Elliott, S. S.; Keim, N. L.; Stern, J. S.; Teff, K.; Havel, P. J. *Am. J. Clin. Nutr.* **2002**, *76*, 911.
15. Asipu, A.; Hayward, B. E.; O'Reilly, J.; Bonthron, D. T. *Diabetes* **2003**, *52*, 2426.
16. Maryanoff, B. E.; O'Neill, J. C.; McComsey, D. F.; Yabut, S. C.; Luci, D. K.; Jordan, A. D.; Masucci, J. A.; Jones, W. J.; Abad, M. C.; Gibbs, A. C.; Petrounia, I. *ACS Med. Chem. Lett.* **2011**, *2*, 538.
17. Gibbs, A. C.; Abad, M. C.; Zhang, X.; Tounge, B. A.; Lewandowski, F. A.; Struble, G. T.; Sun, W.; Sui, Z.; Kuo, L. C. *J. Med. Chem.* **2010**, *53*, 7979.
18. Zhang, X.; Song, F.; Kuo, G.-H.; Xiang, A.; Gibbs, A. C.; Abad, M. C.; Sun, W.; Kuo, L. C.; Sui, Z. *Bioorg. Med. Chem. Lett.* **2011**, *21*, 4762.
19. KHK structure coordinates from in-house studies were used for Glide docking studies. Details on this method are given in Ref. 17.
20. Kinase selectivity was assessed with a panel of 31 kinases, across the kinase families, by using a FRET assay platform from Invitrogen. The kinases were tested with 10 μM compound and 100 μM ATP. Inhibition activities were ranked based on % inhibition at 10 μM. Kinases examined: ABL1, ALK4 (ACVR1B), AKT1, AMPK A1/B1/G1, AURKA, CAMK1D, CAMK2A, CDK1/cyclin B, CHEK1, CHEK2, CSNK1D (CK1δ), DAPK3, EGFR, EPHB1, GSK3B, INSR, IRAK4, JAK2, MAPK13 (p38δ), MST4, NEK2, NTRK1 (TRKA), PAK3, PDGFRB, PIM2, PLK3, PRKACA, PRKCQ (PKCθ), ROCK1, RPS6KA3 (RSK2), SRC. Full names for the kinases are given in the Supplementary data for Ref. 16.